Infrared Spectra of a Species of Astrochemical Interest: Aminoacrylonitrile (3-Amino-2-propenenitrile)

4 AUTHORS:

Abdessamad Benidar
Université de Rennes 1
42 PUBLICATIONS **274** CITATIONS

SEE PROFILE

Jean-claude Guillemin
Ecole Nationale Supérieure de Chimie de Re…
385 PUBLICATIONS **3,359** CITATIONS

SEE PROFILE

Otilia Mó
Universidad Autónoma de Madrid
402 PUBLICATIONS **6,364** CITATIONS

SEE PROFILE

Manuel Yanez
Universidad Autónoma de Madrid
270 PUBLICATIONS **3,735** CITATIONS

SEE PROFILE

Infrared Spectra of a Species of Astrochemical Interest: Aminoacrylonitrile (3-Amino-2-propenenitrile)

Abdessamad Benidar,*,† Jean-Claude Guillemin,*,‡ Otilia Mó,§ and Manuel Yáñez*,§

PALMS, UMR CNRS 6627, Université de Rennes 1, 35042 Rennes, France, Laboratoire de Synthèse et Activation de Biomolécules, UMR CNRS 6052, ENSCR, Institut de Chimie de Rennes, 35700 Rennes, France, and Departamento de Química, C-9 Universidad Autónoma de Madrid (UAM), Cantoblanco, 28049 Madrid, Spain

Ammonia easily reacts on cyanoacetylene in the gas phase or in a solvent to form the *Z*- and *E*-isomers of aminoacrylonitrile (3-amino-2-propenenitrile, **2**). This kinetically stable enamine presents interest for its possible presence in the interstellar medium, the comets, the atmospheres of Planets including the Primitive Earth, and from a theoretical point of view. B3LYP/6-311+G(3df,2p) and G2 calculations indicate that the imine isomer is significantly less stable than the enamine **2**. DFT and G2 calculations indicate that the *Z*-isomer of compound **2** lies ca. 8.0 kJ mol^{-1} lower in energy than the *E*-isomer. The infrared spectra of the aminoacrylonitrile, in both the gas and condensed phases were recorded in the range 500−4000 cm^{-1}. Consistent with the theoretical calculations, the imine and the *E*-isomer of the enamine have never been detected in the infrared spectrum of a gaseous sample and only the *Z*-isomer has been observed. With a neat sample in the condensed phase, IR spectra of a 1:1 and 20:1/*Z:E* mixtures were recorded. The comparison of these data with the spectrum of the *Z*-isomer in the gas phase allowed us to deduce the IR spectrum of the *E*-isomer. The *E*−*Z* isomerization takes place through a torsion around the C≡C bond. A possible mechanism involving a previous enamine−imine tautomerism must be discarded because it implies a much larger barrier than the direct isomerization process. Consistently, the presence of a deuterium atom has not been observed on the *sp*^{2} carbon of the products of distillation of a 1:1/*E:Z* mixture of the NCCH=CHND$_2$.
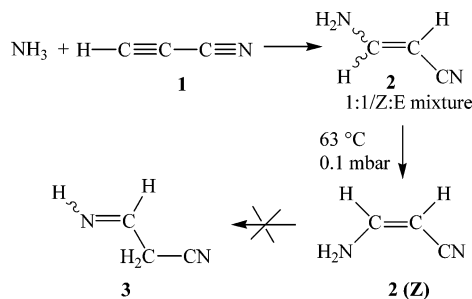
Introduction

Cyanoacetylene (HC≡C−C≡N, **1**) has been observed in the interstellar medium,[1,2] in comets,[3] in the atmosphere of Titan,[4,5] and in numerous lab simulations of planetary atmospheres.[6−8] It was often proposed as a key compound[9,10] because it easily reacts with many nucleophiles and could be the starting point of a rich organic chemistry in these media. Among these nucleophiles, ammonia has been detected in many places in the Universe.[11,12]

The addition of ammonia on cyanoacetylene (**1**) in a solvent[13] or in gaseous phase[14] yields a mixture of *Z*- and *E*-amino-acrylonitrile (**2**) (3-amino-2-propenenitrile). The *Z/E* ratio in the reaction mixture is about 1 but rises to about 20 after distillation in vacuo (Scheme 1).[13]

We observed that compound **2** was stable for several days at room temperature when dissolved in common organic solvents or in water and in the presence of various chemicals (diluted HCl, KCN, methanol, aqueous ammonium chloride, or sodium hydroxide). In all these experiments, the imine isomer has never been detected by analysis of the products in the condensed phase. By comparison, the simplest vinylamine (H$_2$C=CH−NH$_2$) is unstable in the condensed phase on standing at −80 °C[15] and it decomposes in the presence of various chemicals.

---

* Corresponding author. E-mail: jean-claude.guillemin@ensc-rennes.fr. Tel: + (33) (0)2 23 23 80 73. Fax: + (33) (0)2 23 23 81 08.
† PALMS.
‡ ENSCR.
§ UAM.

SCHEME 1

The presence of the carbonitrile substituent on compound **2** dramatically modifies the properties of the enamine.

We report here a theoretical and spectroscopic study on 3-amino-2-propenenitrile (**2**). The reaction pathway of the *Z* ⇆ *E* isomerization, the enamine−imine tautomerism, and the nature of the isomer(s) observed in the gas phase have been determined by theoretical calculations and the compound analyzed by infrared spectroscopy.

Experimental Section

Materials. Cyanoacetylene (**1**) was prepared from the corresponding amide with P$_4$O$_{10}$ and sea sand.[16]

Synthesis of (*Z*+*E*)-3-Amino-2-propenenitrile (2).[13,14] Into a 2 L degassed cell equipped with a stopcock and connected to a vacuum line were successively added the cyanoacetylene (100 mbar) and ammonia (100 mbar). The cell was abandoned for 1

day and yellow-brown oil was observed on the walls of the cell. The gaseous phase was removed in vacuo, and the cell was then washed with dichloromethane (10 mL). The solvent was removed in vacuo. Analysis by ^{1}H NMR spectroscopy of this crude mixture showed a 1:1/*Z:E* ratio of compound **2**. After distillation in vacuo (bp$_{0.1}$ 63 °C), 3-amino-2-propenenitrile (**2**) (479 mg, 7.0 mmol) was obtained as a colorless liquid in an 80% yield and in a 95:5/*Z:E* ratio.

A pure sample of a 1:1/*Z:E* mixture was obtained by addition of few drops of triethylamine on a distilled sample of **2** (200 mg) diluted in dichloromethane (2 mL). After 3 h of stirring at room temperature, the low boiling compounds were removed in vacuo and the sample was analyzed by IR spectroscopy without further purification.

^{1}H NMR spectra of both samples were analyzed before and after recording the IR spectra to check the *Z/E* ratios, which are constant under these conditions.

General Information. [1]H (400 MHz) and ^{13}C (161 MHz) NMR spectra were recorded on a Bruker AC-400P spectrometer. The IR spectra in the gas phase were recorded on a 120HR Bruker Fourier transform interferometer in the range 500−4000 cm^{-1} equipped with a KBr beam splitter, a Globar source, and a liquid nitrogen cooled MCT detector. The spectra (average of 100 scans) were collected at ambient temperature, at a resolution of 1 cm^{-1}. The sample used to record the IR spectrum in the gaseous phase was prepared starting from a 1:1/*Z:E* mixture of 3-amino-2-propenenitrile (**2**). A very small quantity of this compound was vaporized in the multiple path absorption cell. This gas cell with a base path length of 2 m was equipped with the White optical system.[17] To compensate the very weak vapor pressure of this molecule, an adjustment of a total optical path of 96 m was necessary to record its spectrum. This sample vaporized in the cell is kinetically unstable and partially condenses on the walls of the cell or it decomposes. Several successive fillings were required to perform the recording of the spectrum. Consequently, the measurement of the vapor pressure of the gas is a rough approximation, in the range between 0.7 and 1 mbar.

Using the ATR technique, the IR spectra of samples in liquid phase were recorded in the range 500−4000 cm^{-1} on a Vector 22 Fourier transform spectrometer equipped with a ZnSe ATR crystal, a KBr beam splitter and a DTGS detector.

Experimental Determination of the Reaction Pathway for the *Z* ⇌ *E* Isomerization. A 1:1/*Z:E* sample of *N,N*-dideutero-3-amino-2-propenenitrile (**4**) was prepared by addition of 3 mL of methyl alcohol-*d* to 3-amino-2-propenenitrile **2** (0.7 g, 10 mmol). After 10 min of stirring, the low boiling compounds were removed in vacuo. The procedure was repeated four times to obtain compound **4** with an isotopic purity higher than 95%. On the ^{1}H and ^{13}C NMR spectra, the presence of a compound deuterated on the carbon−carbon double bond was not detected. **4** (*E*): ^{1}H NMR (CDCl$_3$) δ 4.26 (d, 1H, $^3J_{HH}$ = 13.8 Hz), 6.99 (d, 1H, $^3J_{HH}$ = 13.8 Hz); ^{13}C NMR (CDCl$_3$) δ 63.7, 122.0, 151.6. **4** (*Z*): ^{1}H NMR (CDCl$_3$) δ 3.95 (d, 1H, $^3J_{HH}$ = 8.4 Hz), 6.77 (d, 1H, $^3J_{HH}$ = 8.4 Hz); ^{13}C NMR (CDCl$_3$) δ 61.4, 118.9, 150.4.

Distillation in vacuo of this sample led to a 20:1/*Z:E* sample of **4**. Once again, we were not able to detect the presence of deuterium on the carbon−carbon double bond.

Computational Details

Standard density functional theory (DFT) calculations have been carried out to obtain the structure, the harmonic vibrational frequencies, and the relative stability of the *E*- and *Z*-isomers of compound **2**. Among the different functionals available nowadays, the B3LYP hybrid method was chosen because its good performance in obtaining reliable geometries and vibrational frequencies is well documented.[18−29] The B3LYP approach includes Becke's three-parameter nonlocal hybrid exchange potential[30] and the nonlocal correlation functional of Lee, Yang, and Parr.[31] For the geometry optimizations, as well as for the calculation of the harmonic vibrational frequencies, the 6-31G(d) basis set expansion has been adopted. To have a reliable estimate of the relative stability of both isomers, the B3LYP/6-31G(d) geometries were refined at the B3LYP/6-31+G(d,p) level and the final energies were obtained in single point B3LYP/6-311+G(3df,2p) on these refined geometries. Because the existence of both isomers in the gas phase is a crucial problem, we have also estimated their relative stabilities through the use of high-level ab initio G2 calculations.[32] All these calculations have been carried out by using the Gaussian-98 series of programs.[33] The same levels of theory were used in the study of the corresponding imine **3**, and their stereo-isomers.

A second-order perturbation NBO analysis[34] has been carried out to gain some insight into the origin of the enhanced stability of the *Z*-isomer with respect to the *E*-isomer. This analysis will be complemented with that performed in terms of the atoms in molecules (AIM) theory.[35] For this purpose we have located the corresponding bond critical points (bcps), whose electron density is a good measure of the strength of the linkage.

Results and Discussion

Structure and Relative Stability. The optimized geometries of both stereoisomers of aminoacrylonitrile **2**, together with their molecular graphs are shown in Figure 1. Their total and relative energies are summarized in Table 1. It can be observed that, no matter the level of theory used, the *Z*-isomer is predicted to be lower in energy than the *E*-isomer. Although this energy gap is small (see Table 1), it is large enough however to predict that the *Z*-isomer would be practically the only one present in the gas phase. More quantitatively, assuming a Boltzmann type distribution and using the relative free energies reported in Table 1, it can be concluded that only 3−5% of the *E*-isomer will be present in the gas phase at 298 K, in nice agreement with the experimental evidence mentioned in preceding sections. This proportion does not change significantly at much lower temperatures (100 K) as the ones expected in Titan's atmosphere. As a matter of fact, as shown in Table 1, the energy gap between both isomers increases only by 0.5 kJ mol^{-1} on going from room temperature (298.2 K) to 100 K.

The reasons for the enhanced stability of the *Z*-isomer are not at all obvious. A topological analysis of its charge density does not reveal the existence of an intramolecular hydrogen bond between the amino and the −CN groups (see Figure 1), which can be easily understood in terms of the unfavorable orientation of the hydrogen bond donor and the hydrogen bond acceptor. There is, however, a very weak interaction between the positively charged hydrogen of the amino group and the negatively charged nitrogen atom of the cyano group, which is reflected in a small decrease of the charge density at the N−H bcp. However, the main difference between both isomers is associated with the conjugation between the amino group and the C=C double bond. As a matter of fact, a second-order perturbation analysis within the framework of the NBO theory shows that in both conformers there is a strong orbital interaction between the lone pair of the amino nitrogen and the π_{CC}* antibonding orbital, which can be viewed as a conjugation of

IR Spectra of Aminoacrylonitrile

J. Phys. Chem. A, Vol. 109, No. 21, 2005 **4707**
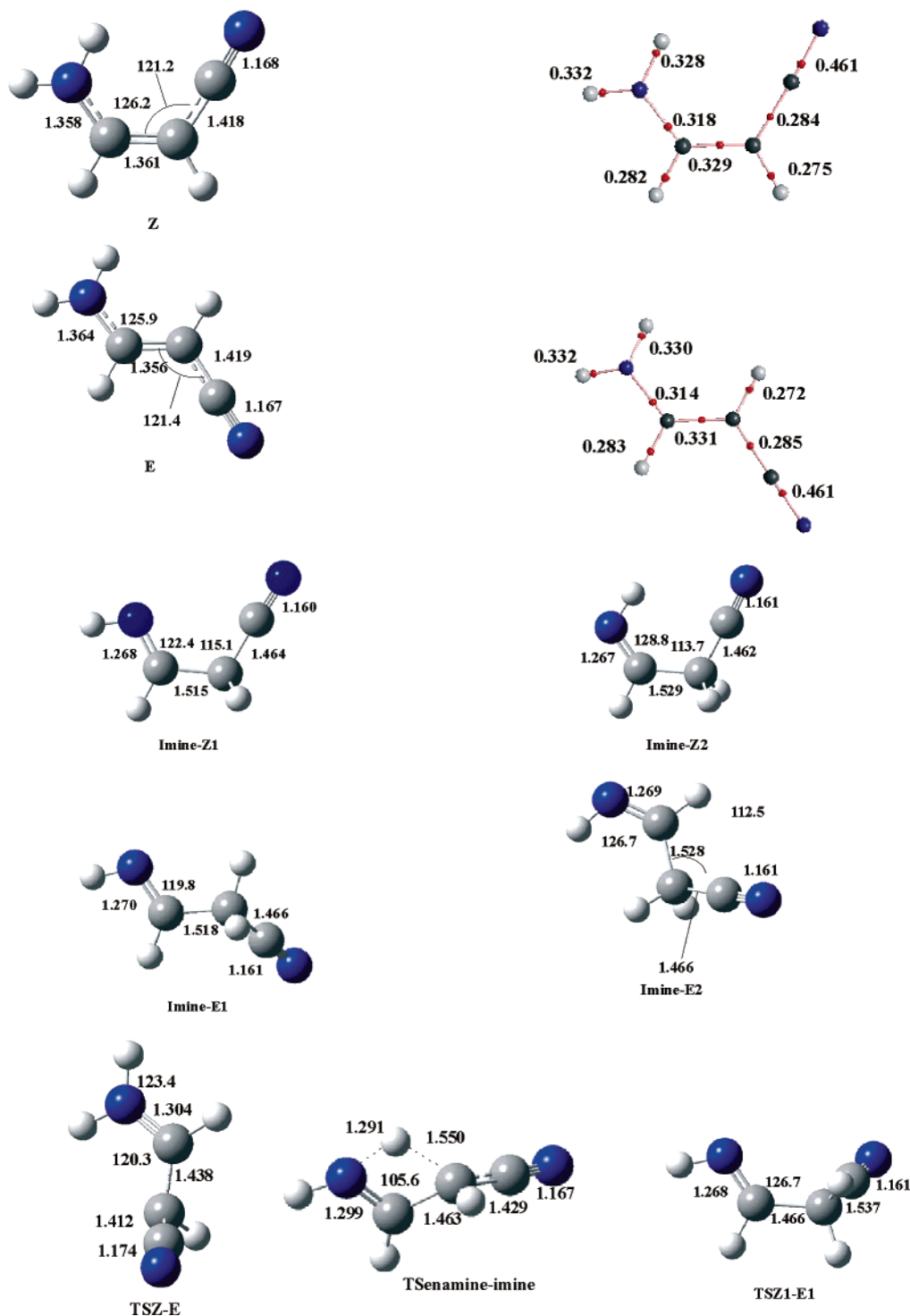
Figure 1. Optimized geometries and molecular graphs of the *E*- and *Z*-isomers of 3-amino-2-propenenitrile. Bond lengths in Å, bond angles in degrees. The charge densities at the bond critical points are in e au^{-3}. The lower part of the figure shows the structures of the *Z*- and *E*-stereoisomers **2** of the imine as well as the transition states connecting *Z*- with *E*-stereoisomers (TSZ-E); the *Z*-enamine with imine-Z1 (TSenamine−imine), and imine-Z1 with imine-E1 (TSZ1-E1).

the amino lone pair with the C=C π-system. However, from a quantitative point of view this interaction is 18 kJ mol^{-1} stronger in the *Z*- than in the *E*-isomer, explaining the enhanced stability of the former. Consistently, the population of the π_{CC}* antibonding orbital is larger in the *Z*- (0.247 electron) than in the *E*-isomer (0.230 electron). Hence, the C=C bond length is longer in the *Z*- (1.361 Å) than in the *E*-isomer (1.356 Å), and the charge density at the bcp is smaller (see Figure 1). Conversely, the C−NH$_2$ bond is shorter in the former (1.358 Å) than in the latter (1.364 Å), in agreement with a better

conjugation between the nitrogen lone pair and the π-system. Again this is reflected in a larger charge density at the C−NH$_2$ bcp in the *Z*- than in the *E*-isomer (see Figure 1). In this respect it is interesting to note that in the *E*-isomer the amino group is slightly pyramidalized, whereas in the *Z*-isomer it is practically planar. This is clearly measured by the deviation from 360° of the sum of the three bond angles around the amino nitrogen. This deviation is 3.3° for the *E*-isomer but only 0.4° for the *Z*-isomer, consistent with a better conjugation of the amino lone pair with the C=C moiety in the case of the latter.

TABLE 1: Calculated Free Energies (*G*, hartrees) and Relative Free Energies (Δ*G*, kJ mol⁻¹) Obtained at 298.2 K

system	B3LYP/6-311+G(3df,2p)		G2	
	G	Δ*G*[a]	*G*	Δ*G*
E	−226.244401	7.5 (8.0)[b]	−225.843132	8.3
Z	−226.247254	0.0 (0.0)[b]	−225.846315	0.0
TSE-Z	−226.166679	211.5 (213.0)[b]	−225.76349	217. 5
ImineZ1	−226.230455	44.1	−225.83586	27.4
ImineE1	−226.232815	37.9	−225.837878	22.1
ImineZ2	−226.230109	45.0		
ImineE2	−226.23168	40.9		
TSenamine−imine	−226.147936	260.8	−225.747668	259.0
TSZ1-E1	−226.226586	54.3	−225.831983	37.6

[a] At the B3LYP/6-31G* level the *Z*-isomer is predicted to be 6.1 kJ mol⁻¹ lower in free energy than the *E*-isomer. [b] Values within parentheses were calculated at 100 K.

SCHEME 2

2 (E)   **3** (E+Z)   **2** (Z)
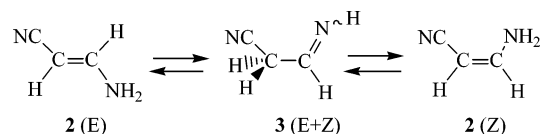
Isomerization Processes. Two different isomerization mechanisms can be envisaged on going from the *E*- to the *Z*-form of compound **2**. The first one would correspond to a direct isomerization process that would imply a C=C torsion. The second one would imply, as a first step, a tautomerization from the enamine to the corresponding imine (see Scheme 2), followed by the interconversion between the *Z*- and *E*-stereoisomers of imine **3** through a torsion of a C−C single bond, which would involve a quite low barrier.

The first question that needs to be addressed to establish which of the aforementioned mechanisms is the most favorable is whether the imine **3** is more or less stable than the enamine tautomer **2**. For this purpose we have used the same levels of theory employed to investigate the enamine stereoisomers. Four different isomers of the imine have been found as local minima of the PES (See Figure 1), two of them are *Z*-conformers (imine-Z1 and Z2) which only differ in the relative position of the imino hydrogen. The other two (imine-E1 and E2) would correspond to the *E*-conformers, although strictly speaking they can be viewed as gauche structures in which the CN group does not lie in the plane of the imino group. More importantly, all of them are found to be significantly less stable than the enamine tautomers (see Figure 2), both at the B3LYP/6-311+G(3df,2p) and G2 levels of theory. This low stability of the imine tautomer is in agreement with the fact, mentioned above, that we could never detect the existence of this form in our experimental investigation of the IR spectra of compound **2**. We have also evaluated the isomerization barriers between both stereoisomers of **2** and between the enamine and the imine tautomers. As shown in Figure 2, the enamine−imine tautomerization process implies an activation barrier 50 kJ mol⁻¹ higher than that corresponding to the C=C torsion that directly connects *Z*- and *E*-isomers of the enamine **2**. This is a quite surprising result because, in general, the enamines rearrange easily to yield the corresponding imines. Hence, to assess that the *Z*−*E* isomerization process does not pass through a previous enamine−imine tautomerization, we have used a 1:1/*Z*:*E* mixture of the NCCH=CHND₂ **4** deuterated species. If after distillation we observe a mixture containing NCCD=CHNDH, we can safely conclude that the enamine−imine tautomerization plays a role in the *Z*−*E* isomerization. If NCCD=CHNDH is the only product, then the *Z*−*E* isomerization will occur exclusively through a previous

enamine−imine tautomerization. In our study we were not able to detect any deuterium exchange, so we must conclude that the enamine−imine tautomerization is either a very minor process or nonexistent, in good agreement with the theoretical predictions.

It is important to note that the *E*−*Z* isomerization barrier is high enough to ensure that indeed both species can be observed in the gas phase. It seems also apparent from the experimental evidence, that the heating of the liquid compound to be distilled provides enough energy to surpass the activation barrier, and although in the condensed phase, both isomers appear in a ratio 1:1, in the gas phase after distillation, the ratio becomes 20:1, in agreement with what should be expected from their relative stabilities. It is worth noting that this situation would not change appreciably at much lower temperatures, because at 100 K the activation barrier is only 1.5 kJ mol⁻¹ larger.

The calculated harmonic vibrational frequencies of both isomers are given in Table 2 and will be used in subsequent sections to assess the assignment of the IR absorption bands.

Analysis of the IR Spectra. The gas phase infrared spectrum of aminoacrylonitrile **2** has been recorded from a 1:1/*Z*:*E* mixture vaporized in the cell up to a pressure of 0.85 ± 0.15 mbar. The spectrum is represented on Figure 3. The fast decomposition of compound **2** in the cell leads to the formation of ammonia, which is easily identified in the spectrum by characteristic absorption bands toward 3336, 1630, and 950 cm⁻¹. Starting from the HITRAN database set,[36] we simulated the IR spectrum of ammonia and, by an adjustment of the intensities of bands according to the experimental conditions, the undesirable bands were subtracted from the spectrum (Figures 4 and 5). Attempts to detect another decomposition product (especially the cyanoacetylene **1**) were unsuccessful.

Only the absorption bands of the *Z*-isomer were observed and identified. This result is consistent with the *E* → *Z* isomerization observed after distillation of the mixture reported above. On the other hand, the spectra of pure liquid 3-amino-2-propenenitrile (**2**) were also recorded. A 1:1 mixture of both isomers and a distilled sample 20:1/*Z*:*E* were used to record the spectra. The spectrum of the *Z*-isomer enabled us to highlight the sensitiveness of different modes to phase changes. Also, the absorption bands of the *E*-isomer were identified. Indeed, in the spectrum of the liquid (1:1/*Z*:*E* mixture), most of the vibration modes present a weak wavenumbers differences between the two respective isomers. Their absorption bands are not quite separated in the spectrum and the shape of the resulting profile does not make easy the identification of the *E*-isomer.

To obtain the spectrum of the *E*-isomer in the liquid phase, we proceeded as follows: the intensities of the absorption bands in the two spectra are adjusted as a function of experimental conditions and are based on the calculated integrated intensities of the absorption bands for each isomer. The spectrum of the *E*-isomer is then obtained by subtraction of the two adjusted spectra. This calculated spectrum is reported in Figure 6.

Assignment of the observed vibrational bands has been carried out by taking advantage of the DFT calculations as indicated in preceding sections. Frequencies of observed and calculated bands are in very good agreement. As it is known, the calculated harmonic vibrational frequencies slightly overestimate the experimental ones. The empirical scale factor between calculated and experimental values for this system ($\nu_{calc(DFT)}/\nu_{obs} = 1.039 \pm 0.005$) is typically of the same order of magnitude as that found in previous papers.[37,38] Table 3 summarizes the assignment of observed bands and gives their relative intensities for the *Z*-isomer in the gas phase.
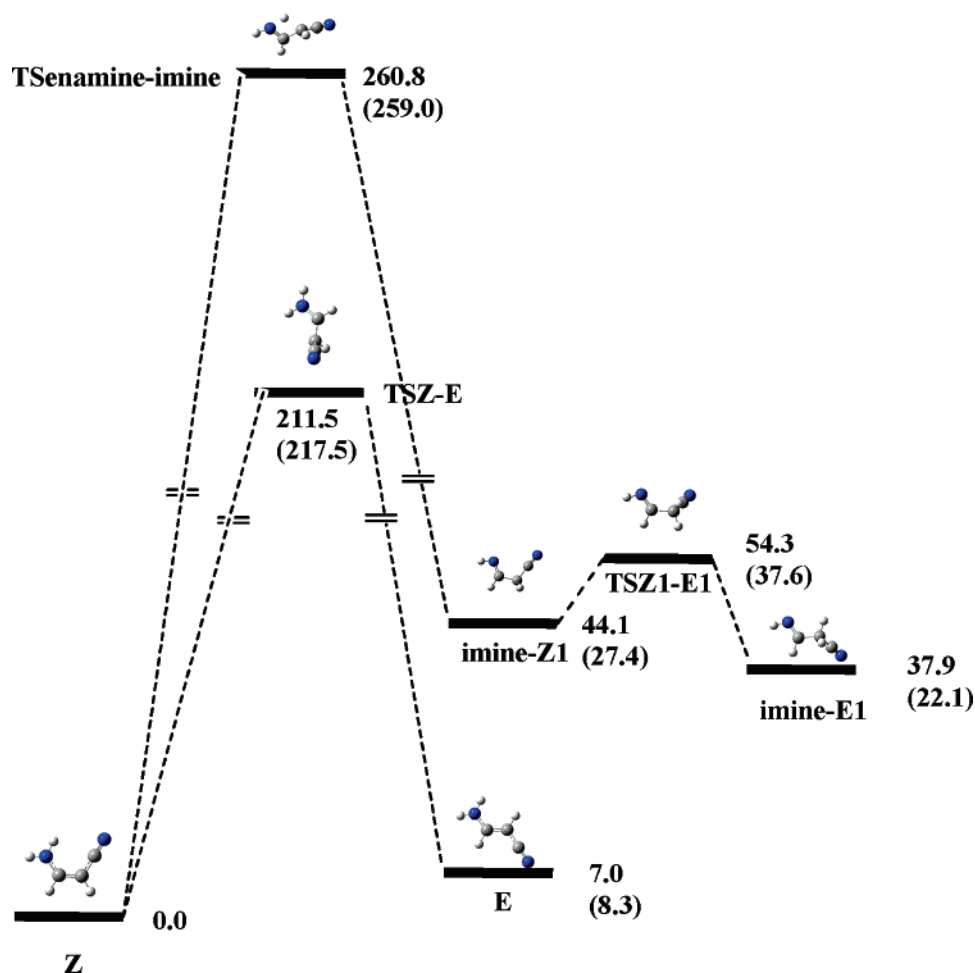
Figure 2. Free energy profiles for the isomerization processes connecting $E-Z$, the Z-enamine and the imine-Z1, and imine-Z1 with imine-E1. B3LYP/6-311+G(3df,2p) energies relative to the Z-isomer are in kJ mol^{-1}. Values within parentheses were obtained at the G2 level of theory.

TABLE 2: Calculated Vibrational Frequencies (cm^{-1}) and Their Intensities Obtained at the B3LYP/6-311G(d) Level for the Z- and E-3-Amino-2-propenenitrile (2)

|	Z-isomer		E-isomer	
assignment	frequency	intensity	frequency	intensity
NH$_2$ asymmetric stretching	37515	43.7	3695.3	32.9
NH$_2$ symmetric stretching	3578.4	41.2	3585.0	55.4
CH stretching (β respect to NH$_2$)	3238.7	3.1	3184.7	7.6
CH stretching (α respect to NH$_2$)	3208.4	6.0	3209.7	4.8
N≡C stretching	2317.7	63.6	2330.2	84.6
C=C stretching (with some NH$_2$ scissors)	1719.6	250.5	1730.2	319.8
NH$_2$ scissoring	1657.8	45.1	1673.1	14.7
CH bending (in-plane and in-phase)	1445.7	0.4	1372.1	13.5
CH bending (in-plane and out-of-phase)	1338.0	65.4	1341.9	12.0
NH$_2$ rocking coupled with C−N stretching	1189.4	0.5	1125.6	4.8
C−N stretching coupled with NH$_2$ rocking	1108.1	18.9	1287.3	90.7
CH bending out-of-plane (α respect to NH$_2$)	973.6	6.2	983.5	23.0
C−C=C bending	968.1	0.8	1006.7	8.4
C=C−N bending in-plane coupled with N≡C−C bending	706.3	4.9	569.6	0.4
CH bending out-of-plane (β respect to NH$_2$)	692.6	38.2	790.1	33.0
N≡C−C bending out-of-plane coupled with NH$_2$ twisting	633.2	35.7	545.5	4.9
NH bending out-of-plane	512.0	58.3	492.2	113.3
N≡C−C bending coupled with C−C−N bending	430.2	7.2	433.3	30.1
NH$_2$ wagging	357.2	235.3	376.9	260.7
skeleton deformation out-of-plane	268.3	35.6	183.1	2.4
skeleton deformation in-plane	140.8	6.6	179.2	1.2

In the gas phase spectrum, the C=C double bond stretching is very intense and absorbs at 1650 cm^{-1}. In vinylic compounds such as X−CH=CH−Y, the double bond of the trans isomers often absorbs at higher wavenumbers than that of the cis isomers and the difference in wavenumber becomes smaller in conju-

gated dienes. For 3-amino-2-propenenitrile, our calculation predicts the same order of absorption between the two isomers with a difference of about 10 cm^{-1}. In the liquid phase spectrum of the mixture, the spectral resolution does not make it possible to identify separately both isomers. They appear under the same
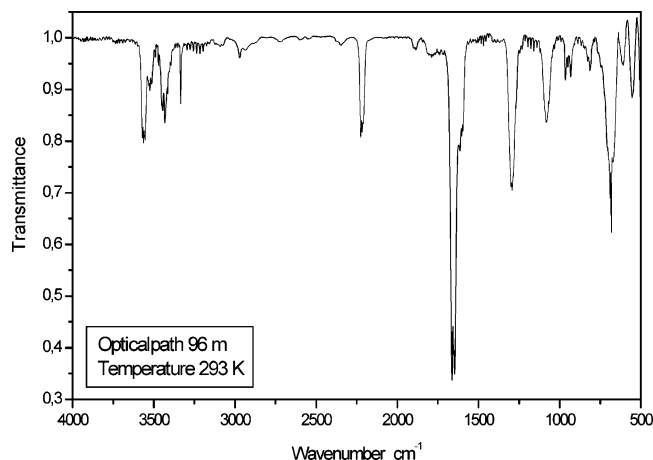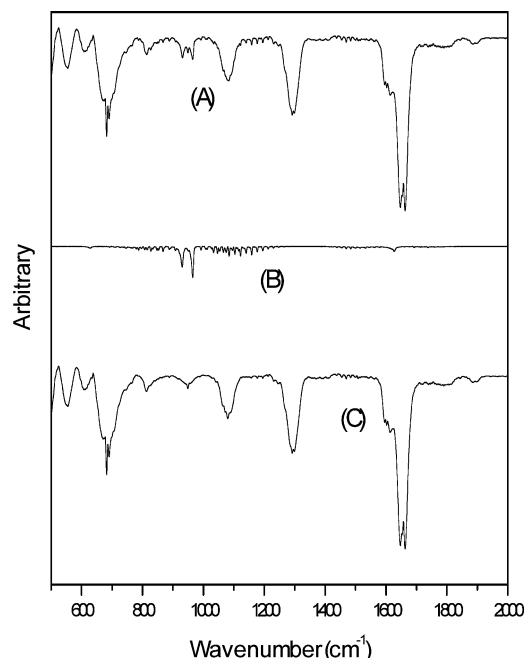
Figure 3. Infrared gas phase spectrum of the 3-amino-2-propenenitrile **2** in the range 500−4000 cm^{-1} using an optical path of 96 m at ordinary temperature.
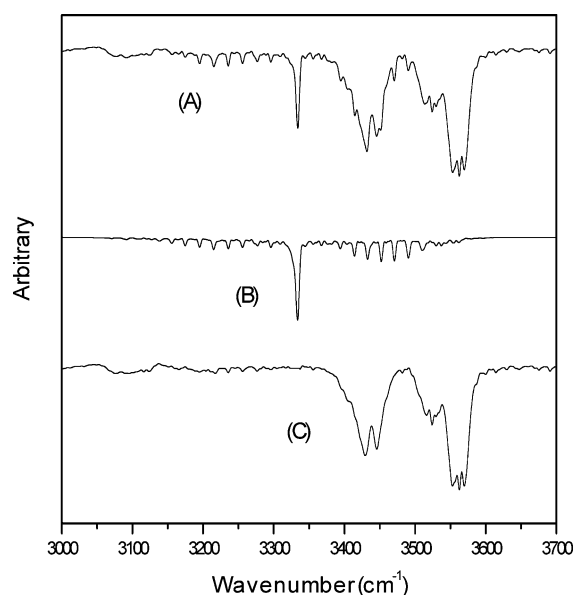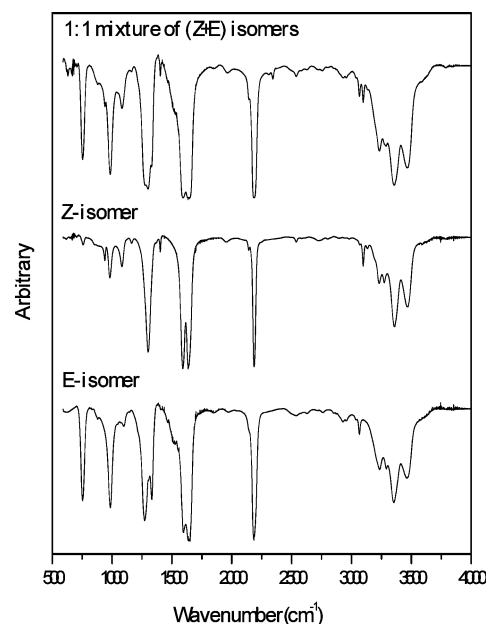

Figure 4. NH stretching range spectrum. (A) Gas phase spectrum of 3-amino-2-propenenitrile (**2**). (B) Simulated NH stretching band of ammonia. (C) Resulting spectrum of *Z*-3-amino-2-propenenitrile after subtraction of traces of ammonia.

Figure 5. NH deformation range spectrum. (A) Gas phase spectrum of 3-amino-2-propenenitrile (**2**). (B) Simulated NH deformation bands of ammonia. (C) Resulting spectrum of *Z*-3-amino-2-propenenitrile after subtraction of traces of ammonia.

Figure 6. Liquid phase spectra. Recorded (*Z*+*E*) mixture of 3-amino-2-propenenitrile (**2**) (upper trace), recorded *Z*-3-amino-2-propenenitrile compound (stereoisomeric purity >95%) (middle trace). Spectrum of the *E*-3-amino-2-propenenitrile obtained by subtraction of the two adjusted-recorded spectra (lower trace).

absorption profile centered at a frequency of 1650 cm^{-1}. A shoulder (1602 cm^{-1}) on the LW side of the observed C=C band in the vapor phase spectrum is attributed to the NH$_2$ scissoring vibration. In the liquid phase this vibration absorbs at the same frequencies for the two isomers, although with different intensities, according to the calculated values. NH$_2$ scissoring presents a characteristic harmonic band enhanced by Fermi resonance near the NH$_2$ stretching vibration region. In solution, the overtone of NH$_2$ scissoring appears on the LW side of the symmetric NH$_2$ stretching. In the vapor phase, the absorption moves to higher wavenumber, becomes sharper, and is well separated. For the *Z*-form, this overtone absorbs at 3524 cm^{-1}.

NH$_2$ stretching vibrations give rise to a nearly symmetrical doublet in the liquid phase. The antisymmetric and symmetric stretching absorb around 3470 and 3370 cm^{-1}, respectively. Differently from the C=C and NH$_2$ scissoring modes, the NH$_2$ stretching modes are very sensitive to the phase change. In the gaseous phase, they appear at higher wavenumber, toward 3562 and 3446 cm^{-1}, for the antisymmetric and the symmetric stretching, respectively. In very good agreement with the DFT

predictions, we found about a 120 cm^{-1} wavenumber difference between the two NH$_2$ stretching modes. One can verify the empirical correlation $\nu_s = 0.682 \ \nu_a + 1023$ given by Krueger.[39]

The two CH stretching vibrations appear in the region around 3000 cm^{-1}. Both CH vibrations, α with respect to NH$_2$ and β with respect to NH$_2$, have very weak intensities, as envisaged by calculations. They absorb at 3116 and 3084 cm^{-1}, respectively, for the gaseous sample. These vibrational modes are not sensitive to the phase effect but vary from one isomer to the other one (see Table 4).

IR Spectra of Aminoacrylonitrile

J. Phys. Chem. A, Vol. 109, No. 21, 2005 **4711**

TABLE 3: Gas Phase Infrared Frequencies (cm⁻¹) and Vibrational Assignments for the Observed Z-3-Amino-2-propenenitrile (2)

assignment[a]	frequency	intensity
NH$_2$ asymmetric stretching	3562.5	m
NH$_2$ scissoring overtone	3524.1	mw
NH$_2$ symmetric stretching	3437.3	m
CH stretching (β respect to NH$_2$)	3116.4	vw
CH stretching (α respect to NH$_2$)	3084.7	vw
N≡C stretching	2217.7	ms
CH bending out-of-plan overtone	1891.0	w
C=C stretching	1654.8	vs
NH$_2$ scissoring	1601.9	m
CH bending (in-plane and in-phase)	1399.0	vw
CH bending (in-plane and out-of-phase)	1291.7	s
NH$_2$ rocking	[1238]	vw
C−N stretching	1070.1	m
CH bending out-of-plane (α respect to NH$_2$)	949.0	w
C−C=C bending	[820]	vw
C=C−N bending	[700]	w
CH bending out-of-plane (β respect to NH$_2$)	690.0	m
N≡C−C bending out-of-plane coupled with NH$_2$ twisting	682.0	m

[a] Qualitative estimation of band intensities is given. Abbreviations: vs, very strong; s, strong; ms, medium strong; m, medium; mw, medium weak; w, weak; vw, very weak. [ ]: tentative assignment.

TABLE 4: Liquid Phase Infrared Frequencies (cm⁻¹) and Vibrational Assignments for the Z- and E-3-Amino-2-propenenitrile (2)[a]

assignment[a]	Z-isomer	E-isomer
NH$_2$ asymmetric stretching	3468	3464
NH$_2$ symmetric stretching	3357	3352
C=C stretching overtone	[3273]	[3289]
NH$_2$ scissoring overtone	3229	3235
CH stretching (β respect to NH$_2$)	3133	3065
CH stretching (α respect to NH$_2$)	3097	3037
N≡C stretching	2186	2186
CH bending out-of-plan overtone	1958	1968
C=C stretching	1638	1643
NH$_2$ scissoring	1598	1596
CH bending (in-plane and in-phase)	1402	1333
CH bending (in-plane and out-of-phase)	1302	1306
NH$_2$ rocking	1163	1101
C−N stretching	1083	1272
CH bending out-of-plane (α respect to NH$_2$)	983	985
C−C=C bending	940	880
C=C−N bending	*	*
CH bending out-of-plane (β respect to NH$_2$)	[673]	[753.0]

[a] [ ]: tentative assignment. *: not assigned.

The CN stretching vibration absorbs at 2217 cm⁻¹ in the gas phase. The intensity of its sharp peak is moderate. It is barely affected by the phase change and is not sensitive to the isomeric effect: in the liquid phase, this mode absorbs at 2191 cm⁻¹ for both the Z- and E- isomers.

Three relatively intense bands were observed between 1400 and 600 cm⁻¹ in the gas phase spectrum. They correspond to the out-of-phase combination of in-plane CH bendings, which absorbs at 1291 cm⁻¹, the C−N stretching, which absorbs with a moderate intensity at 1070 cm⁻¹, and the out-of-plane CH bending (β with respect to NH$_2$), which absorbs at 682 cm⁻¹. In agreement with the theoretical calculations, all the other modes that absorb in this area, namely, CH bending in-plane and in-phase, NH$_2$ rocking, C−C=C bending, and C=C−N bending, have very weak intensities and are hardly visible on the spectrum.

In the liquid phase spectrum, one can notice that these last vibrational modes are not sensitive to the effect of the phase; on the other hand, one observes a more appreciable difference in frequencies (and/or) in intensities between the Z- and E-isomers. No spacing of frequencies was observed between the Z- and E-compounds for the out-of-phase combination of the in-plane CH bendings, which occurs around 1300 cm⁻¹. However, a difference of 70 cm⁻¹ exists in the case of the in-phase combination of the in-plane CH bendings. Also, the out-of-plane CH bending (α with respect to NH$_2$) appears at the same frequency in the two isomers. But, the out-of-plane CH bending (β with respect to NH$_2$) absorbs at 753 cm⁻¹ in the case of E-3-amino-2-propenenitrile, whereas in the case of Z-isomer, this band is shifted about 80 cm⁻¹ toward the red.

The C−N stretching vibration absorbs at 1083 cm⁻¹ for the Z-isomer and at 1272 cm⁻¹ for the E-isomer. The frequency difference observed between the two stereoisomers for the C−N stretching vibration is about 180 cm⁻¹ and the intensity difference is about a factor of 6 in favor of the E-derivative. These values are in very good agreement with the theoretical calculations, which predict a frequency difference of 179 cm⁻¹ and a factor 6 for the intensities.

Conclusion

High level DFT and ab initio calculations indicate that the Z-isomer of aminoacrylonitrile (2) is ca. 8.0 kJ mol⁻¹ more stable than the E-isomer, so that the expected Z/E ratio between both isomers in the gas phase should be 20/1, in good agreement with the experimental findings. These theoretical estimates also indicate that the imine isomer is significantly less stable than the enamine one. Consistently, the imine was never detected in the experiments carried out. The E−Z isomerization takes place through a torsion around the C=C bond. A possible mechanism involving a previous enamine−imine tautomerization must be discarded because it implies a much larger barrier than the direct isomerization process.

The complete assignment of the gas phase infrared spectrum of the Z-isomer has been carried out, profiting the information obtained through appropriate DFT calculations. The infrared spectrum of neat samples of 1:1/ and 20:1/Z:E mixtures of isomers in the condensed phase was also recorded. From these data and those obtained in the gas phase for the Z-isomer, the infrared spectrum of the less stable E-isomer was deduced.

Benidar et al.

References and Notes

(1) Mann, A. P. C.; Williams, D. A. *Nature* **1980**, *283*, 721.

(2) Ungerechts, H.; Warmsley, C. M.; Winnewisser, G. *Astronomy Astrophys.* **1980**, *88*, 259.

(3) Bockelee-Morvan, D.; Lis, D. C.; Wink, J. E.; Despois, D.; Crovisier, J.; Bachiller, R.; Benford, D. J.; Biver, N.; Colom, P.; Davies, J. K.; Gerard, E.; Germain, B.; Houde, M.; Mehringer, D.; Moreno, R.; Paubert, G.; Phillips, T. G.; Rauer, H. *Astronomy Astrophys.* **2000**, *353*, 1101.

(4) Kunde, V. G.; Aikin, A. C.; Hanel, R. A.; Jennings, D. E.; Maguire, W. C.; Samuelson, R. E. *Nature* **1981**, *292*, 686.

(5) Coustenis, A.; Encrenaz, T.; Bézard, B.; Bjoraker, B.; Graner, G.; Dang-Nhu, G.; Arié, E. *Icarus* **1993**, *102*, 240.

(6) Fow, S. W.; Dose, K. *Molecular Evolution and the Origin of Life*; Marcel Dekker Inc.: New York, 1977.

(7) Sanchez, R. A.; Ferris, J. P.; Orgel, L. E. *Science* **1966**, *154*, 784.

(8) Ferris, J. P.; Sanchez, R. A.; Orgel, L. E. *J. Mol. Biol.* **1968**, *33*, 693.

(9) Toupance, G.; Raulin, F.; Buvet, R. *Origins Life* **1975**, *6*, 83.

(10) Orgel, L. E. *Orig. Life Evol. Biosph.* **2002**, *32*, 279.

(11) Wyckoff, S.; Tegler, S.; Engel, L. *Astrophys. J.* **1991**, *368*, 279−286. Huebner, W. F. *Earth, Moon Planets* **2002**, *89*, 179−195.

(12) Marten, A.; Courtin, R.; Gautier, D.; Lacombe, A. *Icarus* **1980**, *41*, 410. Walmsley, C. M. *AIP Conf. Proc.* **1994**, *312*, 463−475.

(13) Xiang, Y.-B.; Drenkard, S.; Baumann, K.; Hickey, D.; Eschenmoser, A. *Helv. Chim. Acta* **1994**, *77*, 2209.

(14) Guillemin, J.-C.; Breneman, C. M.; Josepha, J. C.; Ferris, J. P. *Chem. Eur. J.* **1998**, *4*, 1074.

(15) Mó, O.; Yáñez, M.; Decouzon, M.; Gal, J.-F.; Maria, P.-C.; Guillemin, J.-C. *J. Am. Chem. Soc.* **1999**, *121*, 4653.

(16) Moureu, C.; Bongrand, J. C. *Ann. Chim. Paris* **1920**, *14*, 47.

(17) White, J. U. *J. Opt. Soc. Am.* **1942**, *32*, 285.

(18) Sim, F.; St-Amant, A.; Papai, I.; Salahub, D. R. *J. Am. Chem. Soc.* **1992**, *114*, 4391.

(19) Kim, K.; Jordan, K. D. *J. Phys. Chem.* **1994**, *98*, 10089.

(20) Bauschlicher, C. W. *Chem. Phys. Lett.* **1995**, *246*, 40.

(21) Llamas-Saiz, A. L.; Foces-Foces, C.; Mó, O.; Yáñez, M.; Elguero, E.; Elguero, J. *J. Comput. Chem.* **1995**, *16*, 263.

(22) Bauschlicher, C. W.; Partridge, H. *J. Chem. Phys.* **1995**, *103*, 1788.

(23) Mebel, A. M.; Morokuma, K.; Lin, M. C. *J. Chem. Phys.* **1995**, *103*, 7414.

(24) Montgomery, J. A., Jr.; Frisch, M. J.; Ochterski, J. W.; Peterson, G. A. *J. Chem. Phys.* **1999**, *110*, 2822.

(25) Bertrán, J.; Rodríguez-Santiago, L.; Sodupe, M. *J. Phys. Chem. B* **1999**, *103*, 2310.

(26) Luna, A.; Alcamí, M.; Mó, O.; Yáñez, M. *Chem. Phys. Lett.* **2000**, *320*, 129.

(27) Curtiss, L. A.; Redfern, P. C.; Raghavachari, K.; Pople, J. A. *J. Chem. Phys.* **2001**, *114*, 108.

(28) Alcamí, M.; Mó, O.; Yáñez, M. *Mass Spectrom. Rev.* **2001**, *20*, 195.

(29) Marino, T.; Russo, N.; Toscano, M. *J. Mass Spectrom.* **2002**, *37*, 786.

(30) Becke, A. D. *J. Chem. Phys.* **1993**, *98*, 1372.

(31) Lee, C.; Yang, W.; Parr, R. G. *Phys. Rev. B: Condens. Matter* **1988**, *37*, 785.

(32) Curtiss, L. A.; Raghavachari, K.; Trucks, G. W.; Pople, J. A. *J. Chem. Phys.* **1991**, *94*, 7221.

(33) Frisch, M. J.; Trucks, G. W.; Schlegel, H. B.; Scuseria, G. E.; Robb, M. A.; Cheeseman, J. R.; Zakrzewski, V. G.; Montgomery, J. A., Jr.; Stratmann, R. E.; Burant, J. C.; Dapprich, S.; Millam, J. M.; Daniels, A. D.; Kudin, K. N.; Strain, M. C.; Farkas, O.; Tomasi, J.; Barone, V.; Cossi, M.; Cammi, R.; Mennucci, B.; Pomelli, C.; Adamo, C.; Clifford, S.; Ochterski, J.; Petersson, G. A.; Ayala, P. Y.; Cui, Q.; Morokuma, K.; Malick, D. K.; Rabuck, A. D.; Raghavachari, K.; Foresman, J. B.; Cioslowski, J.; Ortiz, J. V.; Stefanov, B. B.; Liu, G.; Liashenko, A.; Piskorz, P.; Komaromi, I.; Gomperts, R.; Martin, R. L.; Fox, D. J.; Keith, T.; Al-Laham, M. A.; Peng, C. Y.; Nanayakkara, A.; Gonzalez, C.; Challacombe, M.; Gill, P. M. W.; Johnson, B. G.; Chen, W.; Wong, M. W.; Andres, J. L.; Head-Gordon, M.; Replogle, E. S.; Pople, J. A. *Gaussian 98*, Revised A3 ed; Gaussian, Inc.: Pittsburgh, PA, 1999.

(34) Reed, A. E.; Curtiss, L. A.; Weinhold, F. *Chem. Rev.* **1988**, *88*, 899.

(35) Bader, R. F. W. *Atoms in Molecules. A Quantum Theory*; Clarendon Press: Oxford, U.K., 1990.

(36) Database, T. H. m. s. *J. Quant. Spectrosc. Radiat. Transfer* **2003**, *82*, 5.

(37) Benidar, A.; Le Doucen, R.; Guillemin, J.-C.; Mó, O.; Yáñez, M. *J. Mol. Spectrosc.* **2001**, 205, 252−260

(38) Benidar, A.; Le Doucen, R.; Guillemin, J.-C.; Mó, O.; Yáñez, M. *J. Phys. Chem. A* **2002**, *106,* 6262−6270.

(39) Krueger, P. J. *Nature* **1962**, *194*, 1077.